Proc. Natl. Acad. Sci. USA
Vol. 90, pp. 1330–1334, February 1993
Biophysics

Displacement-clamp measurement of the forces exerted by gating springs in the hair bundle

(adaptation/auditory system/hair cell/transduction/vestibular system)

FERNÁN JARAMILLO AND A. J. HUDSPETH

Center for Basic Neuroscience Research, The University of Texas Southwestern Medical Center, Dallas, TX 75235-9039

Contributed by A. J. Hudspeth, November 10, 1992

ABSTRACT **Mechanical stimuli applied to the hair bundle of a hair cell are communicated to the transduction channels by gating springs, elastic elements that are stretched when the bundle is displaced toward its tall edge. To quantify the magnitude and time dependence of the forces exerted by gating springs, we have developed a displacement-clamp system that constrains a bundle's motion while measuring the forces that the bundle produces during adaptation to mechanical stimuli, in response to channel blockage, and upon destruction of the gating springs. Our results suggest that each gating spring exerts a tension of ≈8 pN in the resting bundle and can sustain at least 4–13 pN of additional tension. The experiments provide further evidence that the gating springs account for at least one-third of the hair bundle's dynamic stiffness and that a force of ≈100 fN is sufficient to open a single transduction channel.**

Hair cells are the receptors characteristic of the auditory, vestibular, and lateral-line sensory systems. Each hair cell is a sensitive mechanoreceptor that produces an electrical response when force is applied to the receptive organelle, or hair bundle, that protrudes from the apical cellular surface. A hair bundle is a cluster of a few tens to a few hundreds of elongated processes, termed stereocilia, each of which is stiffened and held erect by a cytoskeleton of cross-linked microfilaments. Because successive stereocilia are progressively longer along a particular transect across the bundle, the bundle's top surface is sloped. Most hair bundles also possess a single true cilium, the kinocilium, that stands adjacent to the tallest stereocilia. Deflection of the elastic hair bundle brings force to bear upon transduction channels located at the bundle's top, causing them to open (for reviews, see refs. 1–3). Force is communicated to the transduction channels by gating springs, elastic links that are stretched when the hair bundle is deflected in the appropriate direction (4–6). These springs are now thought to be tip links, fine filaments that interconnect the tips of adjacent stereocilia (7, 8).

Because of the direct mechanical connection between the hair bundle and the transduction channels, there is a reciprocal relation between bundle stimulation and channel gating (6): just as application of external force to a bundle promotes channel gating, so does opening or closing of the channels exert a force upon the bundle. Measurement of a bundle's mechanical characteristics can, therefore, provide useful information about the transduction process. The gating of transduction channels, for example, manifests itself as a nonlinearity in a bundle's stiffness (6). Adaptation of the transduction process, which continuously adjusts the position at which a bundle is most sensitive (9), involves progressive mechanical relaxation of a deflected bundle (10, 11).

The publication costs of this article were defrayed in part by page charge payment. This article must therefore be hereby marked "*advertisement*" in accordance with 18 U.S.C. §1734 solely to indicate this fact.

In previous studies of hair bundles' mechanical properties, investigators have attached the tip of a flexible glass fiber to a bundle's top. When the fiber's base was then moved, the fiber displaced the bundle (6, 10, 12–15). The stimulus provided by a bent fiber is in general neither a constant force nor a constant displacement. Instead, as the hair bundle moves, the fiber's flexion changes, and the force applied to the bundle also varies. In the present study, we have simplified the analysis of hair-bundle motion by developing a displacement-clamp system. This apparatus permits a bundle to be deflected by a specified amount, or to be held in a particular position, while the requisite force is continuously monitored. The resultant data, which have been presented in preliminary form (16, 17), provide a direct indication of the forces within the resting bundle and those produced in response to mechanical stimulation, adaptation, and channel blockage.

MATERIALS AND METHODS

Preparation. Experiments were conducted on hair cells in the saccular epithelium of the bullfrog *Rana catesbeiana* (18, 19). The otolithic membrane was removed and the preparation was maintained as described (6). A 1-μl drop of Cell-Tak (Collaborative Research) was dried on the coverslip bottom of a 500-μl recording chamber, providing a surface to which the outer surface of the sacculus firmly adhered.

Measurements were conducted on the mechanically stabilized stage of an upright microscope (UEM, Zeiss, Oberkochen, Germany) affixed to an air-suspension table in a vibration-isolated room (20).

Mechanical Stimulation. Each hair bundle was displaced by a flexible glass fiber, 100–200 μm in length and 300–800 nm in diameter, firmly attached to the kinociliary bulb near the bundle's top. Fibers were fabricated and calibrated as described (6, 10); their stiffnesses were 340–1160 $\mu N \cdot m^{-1}$.

A stimulus fiber was moved with a "pi"-type piezoelectrical-bimorph stimulator (21). To prevent resonance of the stimulator, the signal to the bimorph elements was passed through a 16-pole low-pass Bessel filter (model 852, Wavetek, San Diego) with a half-power frequency of 1.1–1.4 kHz. The image of the terminal ≈3 μm of a fiber was magnified ×800 and projected onto a pair of photodiodes in a calibrated displacement monitor (6).

Iontophoresis. Iontophoresis was performed as described (20) with fine-tipped glass microelectrodes, whose resistances were 100–450 MΩ when filled with 500 mM aqueous solutions of either gentamicin sulfate (Sigma) or 1,2-bis(2-aminophenoxy)ethane-*N,N,N',N'*-tetraacetic acid (BAPTA; Molecular Probes). The solutions were supplemented with 25 mM NaCl to prevent polarization of the chlorided silver wire connecting the electrode to the amplifier. Mechanical stim-

Abbreviation: BAPTA, 1,2-bis(2-aminophenoxy)ethane-*N,N,N',N'*-tetraacetic acid.

ulation, iontophoresis, and data collection were controlled by a computer system as described (6, 20).

Displacement Clamp. The displacement-clamp system employed negative feedback to ensure that a hair bundle's position accorded with an external command (Fig. 1). The displacement monitor's output was appropriately scaled and compared with a command signal, and the difference served as an error signal that actuated the piezoelectrical stimulator connected to the fiber's base. The force exerted on the hair bundle was computed from the measured flexion of the stimulus fiber (6, 10, 13).

Performance of the Clamp System. An ideal clamp system would reposition a hair bundle instantaneously in response to a displacement command. The finite bandwidth of the experimental system instead resulted in some slowing of the bundle's motion. When a displacement step was commanded, a hair bundle typically relaxed to its new position with a 10–90% rise time of ≈1 ms. At the outset of the motion, when the fiber and bundle were moving at a rate of ≈40 $\mu m \cdot s^{-1}$, the force trace revealed a transient due to hydrodynamic drag. This transient was of the amplitude, ≈20 pN, expected for a combined drag coefficient near 500 $nN \cdot s \cdot m^{-1}$ (6).

The displacement clamp's performance was also examined by measurement of its frequency response. A waveform synthesizer (model 3325A, Hewlett–Packard) generated a ±35-nm sinusoidal displacement command signal with a flat power spectrum between 1 Hz and 2 kHz. The response of the clamp system, as measured from the power spectrum of the ensuing bundle motion, was approximated by a Lorentzian function with a half-power frequency of ≈200 Hz.

Based upon these and other control experiments, we concluded that the clamp system faithfully effected bundle displacements as large as ±150 nm and measured forces as great as ±150 pN, up to a half-power frequency of at least 100 Hz. With the clamp system in operation, the rms noise in the passband between 3 Hz and 1 kHz was typically 1.5 nm for the displacement monitor and 1.6 pN for the force output.

Sign Conventions. Each displacement or force discussed in this paper lay within a hair bundle's plane of bilateral symmetry. The resting position of the bundle after attachment of the stimulus fiber was defined as zero displacement; in attaching the stimulus fiber, we took care not to impose a static bias on the hair bundle's position. By convention (22), a displacement was positive when in the direction of the bundle's tall edge. Each force reported here was that exerted by the clamp system to move a hair bundle to, or maintain a bundle at, a commanded position. Force was defined as zero when a stimulus fiber was attached to a bundle in its undisturbed position, and a positive force was one directed toward the bundle's tall edge. Positive deflections and forces are displayed upward in all records. Numerical data are presented as means and standard deviations for the indicated numbers of hair cells.

RESULTS

Adaptation. To examine the effectiveness of the displacement-clamp system, we first examined the clamp's ability to detect mechanical changes in hair bundles during a hair cell's adaptation to a protracted stimulus pulse.

When stimulated with a flexible fiber by the conventional technique, a hair bundle displayed a complex time course of movement (Fig. 2*A*). The bundle initially underwent a rapid excursion that was inversely proportional to its dynamic stiffness. The bundle thereafter relaxed farther in the same direction, approaching a plateau displacement with a time constant of 25 ms. This relaxation, which is correlated with adaptation of the mechanoelectrical-transduction process (10, 11), signified a reduction in the hair bundle's chord stiffness (23).

When a hair bundle was deflected under displacement-clamp conditions, the experimental records were strikingly different (Fig. 2*B*). The bundle's position accurately followed the displacement command, while the bundle's dynamic stiffness and subsequent relaxation were reflected in the

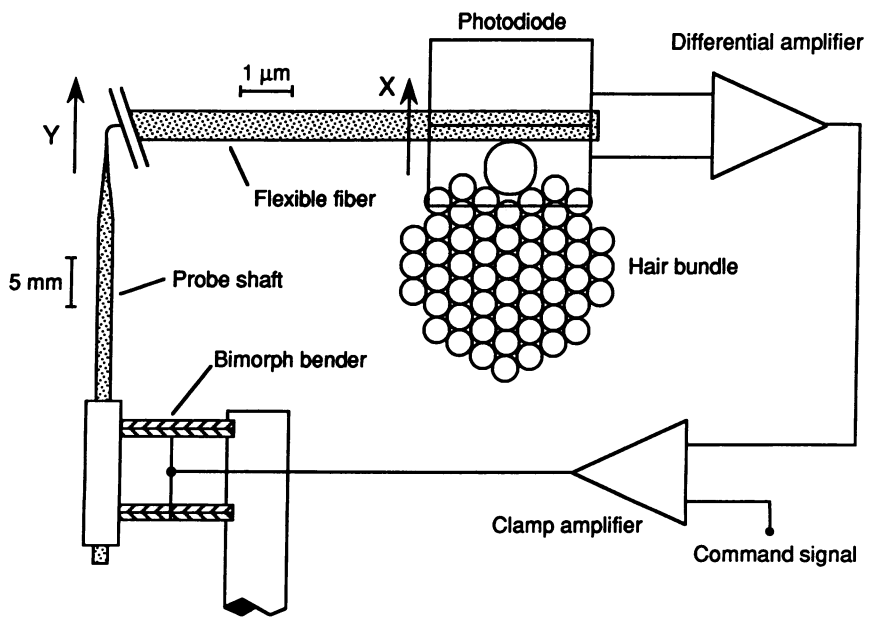

FIG. 1. Displacement-clamp system. The left portion of the drawing represents the piezoelectrical stimulator holding the shank of the stimulus probe. The drawing's top section displays, on a much finer distance scale, the end of the ≈100-μm-long stimulus fiber. The bulbous tip of the kinocilium adhered to the end of the fiber, whose image fell upon a photodiode pair. The remainder of the figure provides a block diagram of the displacement-clamp circuit. A displacement-command signal was delivered to the clamp amplifier, which controlled the voltage applied to the paired piezoelectrical bimorph benders. Flexion of the bimorphs resulted in displacement of the stimulus probe's base through a distance Y and of the fiber's tip and attached hair bundle by a distance X; the force exerted on the bundle by a fiber of stiffness K_F was then $K_F(Y - X)$. Arrows indicate the positive stimulus direction. The tip's movement was monitored as the difference signal from the photodiode pair, which provided feedback to the clamp amplifier to minimize the difference between the commanded displacement and the actual bundle movement.

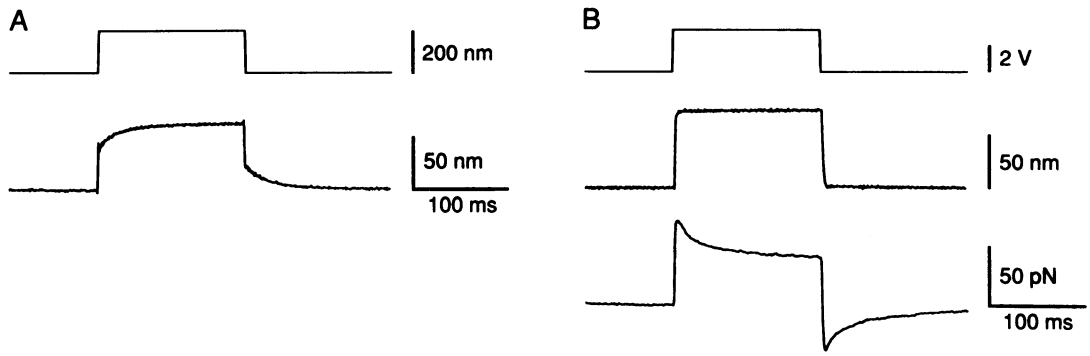

FIG. 2. Base-step vs. displacement-clamp stimulation of a hair bundle. (*A*) Mechanical response of a hair bundle to a 200-nm step displacement of the stimulus fiber's base (upper trace). The bundle's initial stiffness of 1370 $\mu N \cdot m^{-1}$, which was inferred from the displacement of the fiber's tip (lower trace), declined to a steady-state value of 730 $\mu N \cdot m^{-1}$ with a time constant of 25 ms. (*B*) Mechanical response of the same hair bundle when deflected under displacement-clamp conditions. When a command step (top trace) was applied to the clamp amplifier, the hair bundle moved to its final position within 2 ms (middle trace). The force required to displace and hold the hair bundle (bottom trace) indicates that the bundle's stiffness declined with a time constant of 29 ms from an initial value of 1060 $\mu N \cdot m^{-1}$ to a steady-state value of 610 $\mu N \cdot m^{-1}$. Each trace is the average of 16 repetitions; the stimulus fiber's stiffness was 340 $\mu N \cdot m^{-1}$.

force record. Because the bundle did not move after attaining its commanded position, the force trace accurately mirrored the time course of the bundle's stiffness.

We measured the stiffnesses of 12 hair bundles under displacement-clamp conditions. The dynamic stiffness and the steady-state stiffness, respectively, 1040 ± 460 $\mu N \cdot m^{-1}$ and 650 ± 310 $\mu N \cdot m^{-1}$, were similar to the corresponding values obtained in the same cells with the conventional procedure, 1300 ± 610 $\mu N \cdot m^{-1}$ and 750 ± 360 $\mu N \cdot m^{-1}$. For a sample of 12 cells, the time constant of the mechanical relaxation under clamped conditions was 30 ± 18 ms for positive steps of 20–80 nm. This value did not differ significantly from that of 34 ± 12 ms determined after the application to the fiber's base of step displacements that caused initial bundle displacements of 15–64 nm.

Mechanical Effects of Gentamicin. Aminoglycoside antibiotics such as gentamicin are rapid reversible blockers of the mechanoelectrical-transduction channels of hair cells (19). The displacement-clamp system afforded us an opportunity to investigate directly the mechanical consequences of channel blockage. The same experiment also provided a test of a current model for adaptation (refs. 10, 11, and 24; for a review, see ref. 3). It is thought that displacement of a hair bundle in the negative direction closes transduction channels and thus reduces Ca^{2+} entry (9, 25, 26); the adaptation motor then restores tension in the gating springs until the channels reopen. Even in the absence of bundle displacement, blockage of the few channels open at rest would be expected to initiate motor activity by reducing Ca^{2+} influx. Under displacement-clamp conditions, we would then expect to observe the force exerted by the motors.

At the outset of gentamicin iontophoresis onto a hair bundle, the stimulus fiber was required to provide a negative force to maintain the bundle at its resting position (Fig. 3). This negative force, which was observed only when iontophoresis of the drug was efficient and rapid, averaged −4.4 ± 2.4 pN in 15 hair cells. Because this force developed within 2 ms, a latency that reflects the diffusion of drug from the pipette to the channels (20), we believe that it was a direct mechanical consequence of channel blockage.

After the negative force transient, the clamp exerted a positive force that persisted as long as gentamicin remained present (Fig. 3). The sign and duration of this force component accord with the hypothesis that it reflected the activity of adaptation motors activated by Ca^{2+} deprivation. Our measurements from 14 cells indicated that the adaptation motors produced an average force of 29 ± 22 pN, as measured at the hair bundles' tops.

Mechanical Effects of BAPTA. To determine the force that the gating springs exert in the resting hair bundle, we disengaged the springs and measured the force subsequently produced by the hair bundle. Exposing hair bundles to low concentrations of Ca^{2+} abolishes mechanoelectrical transduction (18, 27), evidently by severing or disconnecting the tip links (8). Focal iontophoresis of the Ca^{2+} chelator BAPTA permitted a rapid and local reduction in Ca^{2+} concentration without mechanical artifacts. To facilitate the disruption of tip links, these experiments were performed with only 100 μM Ca^{2+} present in the extracellular saline solution.

At the onset of iontophoretic BAPTA application, the clamp exerted a positive force to hold the hair bundle at its resting position (Fig. 4*A*). We attribute this transient force to the adaptation motors. When the extracellular concentration of unchelated Ca^{2+} falls, Ca^{2+} entry is expected to decline; the motors are consequently expected to increase the tension in gating springs and thus to pull the bundle in the negative direction. This mechanism is the same as that responsible for the positive force observed during application of gentamicin (Fig. 3).

As BAPTA application continued for a few hundred milliseconds, the force exerted by the clamp system reversed sign and reached a plateau (Fig. 4*A*). This component, which persisted indefinitely, evidently resulted from loss of the tip links, whose resting force on the bundle was thereafter assumed by the clamp system. If all the tip links are broken by BAPTA, we estimate from observations on 12 cells that the gating springs provide a force of −57 ± 35 pN in the undisplaced bundle.

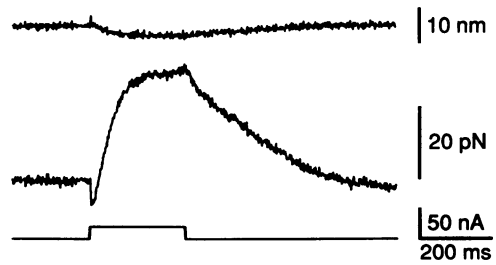

FIG. 3. Mechanical effects of gentamicin. A 250-ms 19-nA iontophoretic pulse (bottom trace) was passed through an electrode situated within 5 μm of a hair bundle. The force signal (middle trace) revealed a rapidly developing transient of −5.7 pN, followed by a sustained force of 32 pN. The hair bundle, which was commanded to remain stationary, moved by less than ±3 nm during the drug's application (top trace); the forces were consequently underestimated by <7%. Each trace is the average of 10 repetitions.

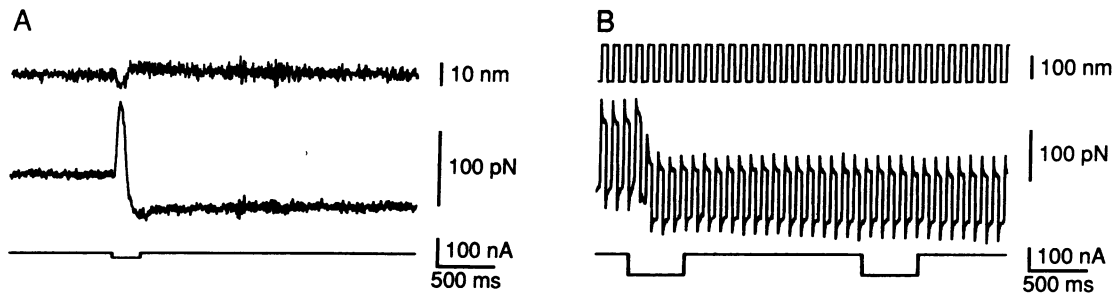

FIG. 4. Mechanical effects of BAPTA. (*A*) As an iontophoretic electrode delivered a 500-ms −19-nA current pulse (bottom trace), the clamp system held the hair bundle stationary (top trace). The force signal (middle trace) showed a transient of 96 pN followed by the irreversible appearance of a −53-pN force. Because the bundle moved by less than ±5 nm, these values represent underestimates by at most 4%. (*B*) The displacement clamp was driven with a 10-Hz pulse command that resulted in a peak-to-peak bundle movement of 165 nm (top trace). The force required to produce this motion (middle trace) declined by ≈30% after the initial iontophoretic application of BAPTA, signaling a decrease in the hair bundle's dynamic stiffness from 840 $\mu N \cdot m^{-1}$ to 570 $\mu N \cdot m^{-1}$. The forces resulting from the pulse commands were superimposed upon force components similar to those in *A*. The amplitude of the iontophoretic pulse (bottom trace) was −90 nA; a second such pulse had no further effect.

In other experiments we applied BAPTA while commanding the hair bundle to follow a repetitive pattern of 125- to 165-nm displacement pulses (Fig. 4*B*). After BAPTA application, we again observed the development of a transient force in the positive direction, followed by the irreversible appearance of a negative force. The force pulses necessary for the clamp system to effect the commanded displacements indicated that bundle stiffness declined after BAPTA treatment. In seven hair cells, the dynamic bundle stiffness was initially 1340 ± 340 $\mu N \cdot m^{-1}$; immediately after BAPTA application, the stiffness fell to 970 ± 330 $\mu N \cdot m^{-1}$.

DISCUSSION

The Displacement Clamp. Clamp systems simplify the analysis of complex physiological processes by permitting experimenters to hold one variable constant, or to alter it in a systematic way, while analyzing the effects on a second variable. The displacement-clamp system described here has enabled us to examine the responses of hair bundles to well controlled displacement stimuli and to measure directly the forces produced within bundles in response to various manipulations.

Components of Hair-Bundle Stiffness. Our results provide two means of estimating the contribution of gating springs to a hair bundle's stiffness. If adaptation were complete, so that gating springs bore the same tension in the resting and the fully adapted states, then the stiffness contribution of the gating springs would be given by the difference between the dynamic and steady-state stiffnesses. Based on this approximation, the displacement-clamp data indicate that gating springs contribute 390 $\mu N \cdot m^{-1}$ to a bundle's dynamic stiffness. In view of the experimental uncertainty, this value is in agreement with that of 550 $\mu N \cdot m^{-1}$ obtained by use of the conventional stimulation technique on the same hair cells.

The removal of gating springs by BAPTA provides a second independent means of assessing the relative contributions to a bundle's stiffness of the gating springs and stereociliary pivots. If BAPTA quantitatively severs or disconnects the gating springs and if it has no significant effects on other bundle components, then the difference between the dynamic stiffnesses of intact and BAPTA-treated bundles should indicate the contribution of the gating springs. Our data from this experiment suggest that the springs contribute an average of 370 $\mu N \cdot m^{-1}$ to a bundle's stiffness at rest.

If the tip links are the gating springs, then N links, each of stiffness κ_{GS}, will contribute to the bundle's stiffness (1, 6) a component, K_{GS}, given by

$$K_{GS} = N\gamma^2\kappa_{GS}, \quad [1]$$

in which γ is the geometrical gain, due to the disposition of the gating springs within the hair bundle, that relates a change in gating-spring length to a given displacement of the bundle's top. If the tip links are the gating springs, $\gamma \approx 0.14$ (6). For a hair cell with ≈50 tip links (5, 6) contributing to a stiffness component of ≈390 $\mu N \cdot m^{-1}$, the displacement-clamp results imply that each link has a stiffness of ≈400 $\mu N \cdot m^{-1}$. This estimate is comparable to those made earlier on the basis of conventional stimulation (6, 10).

The component of hair-bundle stiffness that cannot be attributed to gating springs presumably resides in the stereociliary pivots (13, 14). If the basal and apical-lateral linkages of stereocilia (for review, see ref. 2) restrict sliding between apposed processes, they would also contribute to this term. The present data indicate that the combined stiffness of the pivots is ≈650 $\mu N \cdot m^{-1}$, or ≈11 $\mu N \cdot m^{-1}$ for each of the 60 or so stereocilia in a large bundle (23). The relative stiffnesses of the gating springs and stereociliary pivots imply that about one-third of the work done in deflecting the bundle is focused on the gating springs, where it can contribute to channel gating.

Mechanical Effect of Channel Blockage. The initial effect of gentamicin application was a transient force of −4.4 pN, indicative of a decline in the tension borne by the gating springs. Such a decrease would be expected if gentamicin traps channels with their gates in an open position. Applied at sufficiently high concentrations, gentamicin would then shift the opening-and-closing equilibrium entirely toward the open (but blocked) state. A similar interpretation has been offered for the positive bundle motion previously documented in unrestrained bundles (28).

The force that the clamp furnishes to immobilize a hair bundle during the gentamicin transient permits estimation of the single-channel gating force, z, which must be applied to the bundle's top to open a single transduction channel. If ΔF is the change in the force produced by N channels when the drug is applied, then it may be shown (1, 23) that

$$z = -\Delta F[N(p_2 - p_1)]^{-1}. \quad [2]$$

Here p_1 and p_2 are the probabilities of finding a channel in the open state preceding and following the application of gentamicin. The probabilistic factor arises because no change in tension is expected when gentamicin fails to block a channel or when it blocks one that is open at rest. If we assume that a bundle contains ≈50 channels and that $p_1 \approx 0.15$ (for review, see ref. 2) and if all channels are blocked by the concentration of gentamicin applied in our experiments, then $z \approx 100$ fN. This value is about one-third previous estimates obtained from the Boltzmann distribution relating channel

open probability to bundle displacement, which range up to 290 fN (6). The present estimate of z could be low, however, because gentamicin destroyed some tip links (29), because the drug did not completely block the channels, or because a blocked channel's gate could partially close.

Tension in the Gating Springs. Previous evidence suggested that the gating springs are under tension when a hair bundle is at rest (for review, see ref. 23); the gating springs pull upon the stereocilia like the taut string on a strung bow. When the tip links are disrupted by the application of the Ca^{2+} chelator BAPTA, a stimulus fiber must produce a force of -57 pN to retain a hair bundle at its resting position. We believe that this negatively directed force is exerted against strained actin fascicles in the stereociliary pivots (13, 14), whose effect becomes apparent when the gating springs become disengaged and no longer exert a countervailing force on the stereociliary tips. If the stereociliary pivots have a combined stiffness of $\approx 650\ \mu N \cdot m^{-1}$, a force of -57 pN should draw a resting bundle ≈ 88 nm in the negative direction. Because BAPTA treatment allows an unrestrained hair bundle to lurch an average of 133 nm in the positive direction (8), the resting tension may be even greater.

The effects of gentamicin and BAPTA indicate that the gating springs are capable of sustaining substantial tension in excess of the resting level. During sustained gentamicin application, the clamp exerted an average force of 29 pN to restrain hair bundles. At the onset of exposure to BAPTA, a bundle could produce a peak force as great as 96 pN. We attribute these forces to the molecular motors responsible for maintaining the resting tension in the gating springs. These motors are normally activated by a fall in the intracellular Ca^{2+} concentration due to channel closure upon negative stimulation (10, 11, 25, 26). By respectively occluding the channels and chelating extracellular Ca^{2+}, gentamicin and BAPTA also reduce Ca^{2+} entry and initiate motor activity.

Our results indicate that the gating springs are capable of exerting a total force on the hair bundle, including both the resting force and that evoked by gentamicin or BAPTA, of at least 86 pN, and probably as much as 149 pN. The force F experienced by the bundle due to the concerted action of N gating springs, each of which contributes a force f, is given by

$$F = N\gamma f, \qquad [3]$$

in which γ is again the bundle's geometrical gain (1). If the tip links are the gating springs and if each hair cell has ≈ 50 active transduction channels (5, 6), we then conclude that the tension in each link can exceed at least 12 pN and perhaps as much as 21 pN.

The tension borne by each tip link sets a lower limit on the force that can be produced by the apparatus responsible for adaptation. If a myosin I-based motor regulates the tension in a tip link (10, 11, 24, 30) and if an individual myosin molecule produces a maximal force of ≈ 1 pN (31), then the adaptation motor connected to each link must comprise at least one or two dozen myosin molecules. The most probable site for such a motor, the osmiophilic plaque at the upper insertion of each tip link, is 40–50 nm in diameter (32). Because such a structure could accommodate as many as 20–100 myosin I heads, each 5–8 nm in diameter (33, 34), this insertional plaque could potentially exert forces of the magnitude required by the displacement-clamp data.

Mr. R. A. Jacobs carefully stabilized the microscope, fabricated the mechanical stimulator and photodiode assembly, and produced the figures; Dr. J. Howard provided apparatus and valuable computer programs. For critical comments on the manuscript, we thank Mmes. E. A. Lumpkin and A. B. Metcalf; Messrs. M. E. Benser, N. P. Issa, R. A. Jacobs, K. P. Rosenblatt, and R. G. Walker; and Drs. J. L. Allen, R. Fettiplace, P. J. Foreman, P. G. Gillespie, and V. S. Markin. This research was supported by National Institutes of Health Grant DC00317.

1. Howard, J., Roberts, W. M. & Hudspeth, A. J. (1988) *Annu. Rev. Biophys. Biophys. Chem.* **17**, 99–124.
2. Roberts, W. M., Howard, J. & Hudspeth, A. J. (1988) *Annu. Rev. Cell Biol.* **4**, 63–92.
3. Hudspeth, A. J. (1989) *Nature (London)* **341**, 397–404.
4. Corey, D. P. & Hudspeth, A. J. (1983) *J. Neurosci.* **3**, 962–976.
5. Holton, T. & Hudspeth, A. J. (1986) *J. Physiol. (London)* **375**, 195–227.
6. Howard, J. & Hudspeth, A. J. (1988) *Neuron* **1**, 189–199.
7. Pickles, J. O., Comis, S. D. & Osborne, M. P. (1984) *Hearing Res.* **15**, 103–112.
8. Assad, J. A., Shepherd, G. M. G. & Corey, D. P. (1991) *Neuron* **7**, 985–994.
9. Eatock, R. A., Corey, D. P. & Hudspeth, A. J. (1987) *J. Neurosci.* **7**, 2821–2836.
10. Howard, J. & Hudspeth, A. J. (1987) *Proc. Natl. Acad. Sci. USA* **84**, 3064–3068.
11. Howard, J. & Hudspeth, A. J. (1987) in *Sensory Transduction*, eds. Hudspeth, A. J., MacLeish, P. R., Margolis, F. L. & Wiesel, T. N. (Fondation pour l'Etude du Système Nerveux Central et Périphérique, Geneva), pp. 138–145.
12. Flock, Å. & Strelioff, D. (1984) *Nature (London)* **310**, 597–599.
13. Crawford, A. C. & Fettiplace, R. (1985) *J. Physiol. (London)* **364**, 359–379.
14. Howard, J. & Ashmore, J. (1986) *Hearing Res.* **23**, 93–104.
15. Russell, I. J., Richardson, G. P. & Kössl, M. (1989) *Hearing Res.* **43**, 55–70.
16. Jaramillo, F. & Hudspeth, A. J. (1992) *Biophys. J.* **61**, A516 (abstr.).
17. Jaramillo, F. & Hudspeth, A. J. (1992) *Soc. Neurosci. Abstr.* **18**, 1399 (abstr.).
18. Hudspeth, A. J. & Corey, D. P. (1977) *Proc. Natl. Acad. Sci. USA* **74**, 2407–2411.
19. Kroese, A. B. A., Das, A. & Hudspeth, A. J. (1989) *Hearing Res.* **37**, 203–218.
20. Jaramillo, F. & Hudspeth, A. J. (1991) *Neuron* **7**, 409–420.
21. Corey, D. P. & Hudspeth, A. J. (1980) *J. Neurosci. Methods* **3**, 183–202.
22. Shotwell, S. L., Jacobs, R. & Hudspeth, A. J. (1981) *Ann. N.Y. Acad. Sci.* **374**, 1–10.
23. Hudspeth, A. J. (1992) in *Sensory Transduction*, eds. Corey, D. P. & Roper, S. D. (Rockefeller Univ. Press, New York), pp. 357–370.
24. Assad, J. A. & Corey, D. P. (1992) *J. Neurosci.* **12**, 3291–3309.
25. Assad, J. A., Hacohen, N. & Corey, D. P. (1989) *Proc. Natl. Acad. Sci. USA* **86**, 2918–2922.
26. Hacohen, N., Assad, J. A., Smith, W. J. & Corey, D. P. (1989) *J. Neurosci.* **9**, 3988–3997.
27. Crawford, A. C., Evans, M. G. & Fettiplace, R. (1991) *J. Physiol. (London)* **434**, 369–398.
28. Denk, W. (1989) Ph.D. thesis (Cornell University, Ithaca, NY).
29. Pickles, J. O., Comis, S. D. & Osborne, M. P. (1987) *Hearing Res.* **29**, 237–244.
30. Gillespie, P. G. & Hudspeth, A. J. (1992) *Soc. Neurosci. Abstr.* **18**, 1398 (abstr.).
31. Huxley, A. F. & Simmons, R. M. (1971) *Nature (London)* **233**, 533–538.
32. Jacobs, R. A. & Hudspeth, A. J. (1990) *Cold Spring Harbor Symp. Quant. Biol.* **55**, 547–561.
33. Howe, C. L. & Mooseker, M. S. (1983) *J. Cell Biol.* **97**, 974–985.
34. Conzelman, K. A. & Mooseker, M. S. (1987) *J. Cell Biol.* **105**, 313–324.